Ceramics-Silikáty 60 (2), 27-33 (2016)
journal webpage: www.ceramics-silikaty.cz doi: 10.13168/cs.2016.0004

PREPARATION OF Al_2O_3–$CaAl_{12}O_{19}$–ZrO_2 COMPOSITE CERAMIC MATERIAL BY THE HYDRATION AND SINTERING OF $Ca_7ZrAl_6O_{18}$-REACTIVE ALUMINA MIXTURE

#DOMINIKA MADEJ, JACEK SZCZERBA

AGH University of Science and Technology, Faculty of Materials Science and Ceramics, al. A. Mickiewicza 30, 30-059 Krakow, Poland

#E-mail: dmadej@agh.edu.pl

Submitted October 31, 2015; accepted February 9, 2016

Keywords: Calcium zirconium aluminate, Reactive alumina, Hydration, X-ray diffraction analysis, Calcium hexaaluminate

Ceramic material of composition belonging to the Al_2O_3–$CaAl_{12}O_{19}$–ZrO_2 compatibility field was obtained as a result of hydration and sintering of the mixture of Al_2O_3 and $Ca_7ZrAl_6O_{18}$ powders. The hydrated Al_2O_3–$Ca_7ZrAl_6O_{18}$ mixture products were studied by XRD, DTA-TG-EGA and FT-IR after 14 days of curing and hydration at 50°C. C_3AH_6, $Al(OH)_3$ and $CaZrO_3$ compounds were formed upon hydration. $CaZrO_3$ and the lime-rich calcium aluminates formed as transient phases during hydration and dehydration processes were converted to CA_6 and ZrO_2 in the presence of an excess of Al_2O_3 during sintering at 1500°C. The Al_2O_3-based dense refractory composite material was investigated by XRD, FT-IR, SEM-EDS and mercury porosimetry. The sintered ceramic microstructure consists of a homogeneous distribution of zirconia grains in an alumina matrix reinforced with the calcium hexaaluminate phase. The presence of Al_2O_3, $CaAl_{12}O_{19}$ and ZrO_2 in the synthesized material was confirmed by XRD and FT-IR techniques. By applying the mercury intrusion porosimetry technique, the heterogeneous pore size distribution of the refractory composite material was determined.

INTRODUCTION

The phase diagram of the system CaO-Al_2O_3, and its binary compounds, was studied extensively in the past because of the interest especially in the production of calcium aluminate cements (CACs) [1-4]. Because of the high melting temperatures in this system, and due to the hydraulic properties of some calcium aluminates, CACs are successfully used in the corundum refractory castables [5-6]. Among the binary phases in the CaO–Al_2O_3 system [7], e.g. $Ca_3Al_2O_6$, $Ca_{12}Al_{14}O_{33}$, $CaAl_2O_4$, $CaAl_4O_7$, and $CaAl_{12}O_{19}$, calcium heksaaluminate $CaAl_{12}O_{19}$ has the highest melting point (1849°C) but it has no reaction with water. Calcium monoaluminate, $CaAl_2O_4$, that melts incongruently at 1604°C, is the majority component of high alumina cement. Commercial CACs are known to contain minor phases $CaAl_4O_7$ (1764°C), $Ca_{12}Al_{14}O_{33}$ (1425°C) and α-Al_2O_3 (2050°C).

One of the most important aspects of CACs chemistry is constituted by the hydration process [8-9]. The calcium aluminates in CACs react with water to form calcium aluminate hydrates of various possible forms, depending on the water-solid ratio, time and temperature of hydration [5, 10-11]. The following calcium aluminate hydrate phases may be formed in the hydration of calcium aluminates: CAH_{10}, C_2AH_8, C_3AH_6, C_4AH_x (C≡CaO, A≡Al_2O_3, H≡H_2O), and crystalline $Al(OH)_3$ or amorphous aluminate hydrate gel (AH_3-gel) [12]. At 50°C, or above other ternary phases are rapidly replaced by cubic C_3AH_6, the only calcium aluminate hydrate which is thermodynamically stable at ambient temperature [13].

In the CaO–ZrO_2–Al_2O_3 system, the ternary compound, i.e. calcium zirconium aluminate, $Ca_7ZrAl_6O_{18}$, that shows incongruent melting point at 1550°C, has been found by Berezhnoi and Kordyuk [14]. $Ca_7ZrAl_6O_{18}$ is a hydratable compound [15-19] that reacts with water to yield calcium aluminate hydrates (C–A–H), aluminium hydroxide and calcium zirconate, $CaZrO_3$. The degree of hydration of $Ca_7ZrAl_6O_{18}$ is determined by water addition, temperature and time [18]. The hydrogarnet phase (C_3AH_6), a crystalline form of aluminium hydroxide ($Al(OH)_3$) and $CaZrO_3$, was the product from the hydration of $Ca_7ZrAl_6O_{18}$ at 60°C [18]. The hydrates CAH_{10}, C_2AH_8 and C_4AH_{19}, obtained at lower temperatures [16-17], are metastable phases that transform with time to more stable and denser cubic hydrogarnet C_3AH_6. The hydration products of $Ca_7ZrAl_6O_{18}$ were similar to those formed in the hydration reaction of CACs. In low cement castables (LCCs), the calcium aluminate cement is replaced by hydratable aluminas [6]. This is, the way to reduce the lime content of the refractory concrete.

The aim of this study is to characterize the reaction and phases of the cementitious materials: reactive alumina (Al_2O_3) and calcium zirconium aluminate ($Ca_7ZrAl_6O_{18}$) at two temperatures (50°C and 1500°C). This is an important issue for a possible application of $Ca_7ZrAl_6O_{18}$ as a binding material in the high alumina castables technology.

EXPERIMENTAL

Solid way synthesis procedure of calcium zirconium aluminate ($Ca_7ZrAl_6O_{18}$) and methods of investigation

Calcium zirconium aluminate was prepared by the solid state reaction method using calcium carbonate ($CaCO_3$, 98.81 % Chempur), aluminum oxide (Al_2O_3, 99.7 % Acros Organics) and zirconium oxide (ZrO_2, 98.08 % Merck) as the starting materials. The specific molar ratio of calcium oxide, aluminum oxide, and zirconium oxide ($CaO:Al_2O_3:ZrO_2$) was 7:3:1, respectively. The reactants were thoroughly milled together, using the conventional ball milling apparatus for 2 h. The milled powders were then pressed into cylindrical green pellets of 20 mm in diameter and comparable height at 30 MPa and were pre-sintered at 1300°C for 10 h in air using the electric furnace. The calcined products were crushed and ground using a mortar and pestle, followed by sieving using the 60 μm test sieve to obtain better powder homogenity. The sieved powders were compacted again into disk-shaped samples (pellets) with a 20 mm diameter under a pressure of 30 MPa. The compacted pellets were subsequently sintered at 1500°C for 30 h in air, cooled together with the furnace and powdered. The formation of the crystalline phases of the sintered samples was analyzed by X-ray diffractometry (XRD) at room temperature using the PANalytical X'Pert Pro MPD diffractometer system with Cu Kα radiation from to 5° to 90° at 2θ intervals. The grain size distribution of cementitious materials i.e. the synthesized calcium zirconium aluminate ($Ca_7ZrAl_6O_{18}$) and commercially available reactive alumina (Al_2O_3, Alteo-P172SB) powders was examined by dynamic light scattering (DLS) techniques (Malvern Mastersizer 2000).

Preparation of the reactive alumina-$Ca_7ZrAl_6O_{18}$ anhydrous and hydrating mixtures and methods of investigation

The anhydrous mixture of Al_2O_3 and $Ca_7ZrAl_6O_{18}$ powders was prepared by conventional mixing of reactive alumina with the addition of 10 % by weight of the synthesized $Ca_7ZrAl_6O_{18}$ phase. The powder mixture was homogenized during a 1-hour period of continuous mixing. As the next step, thirty three grams of mixture of hydratable alumina and calcium zirconium aluminate ($A–C_7A_3Z$) was mixed with 10 g of distilled water. One hydration condition was employed, i.e. hydration for 14 days at 50°C in a sealed polyethylene bag above 80% relative humidity. The phase composition of the unhydrated ($A–C_7A_3Z$; $Z≡ZrO_2$) and hydrated ($A–C_7A_3Z–H$) samples was determined by X-ray diffraction. The infrared spectra (FT-IR) of the samples were recorded in the spectral range of 4000 - 400 cm^{-1} after 128 scans at 4 cm^{-1} resolution with the help of the Fourier BIO-RAD FTS60 V spectrometer. The samples were analyzed as KBr pellets. The hydration extent of the hydrated sample was investigated using simultaneous TG, DTA and EGA technique (NETZSCH STA 449 F3 Jupiter) at a heating rate of 10°C·min^{-1} under a flow of N_2/O_2 (20 ml·min^{-1}), using α-Al_2O_3 as a standard. Before XRD, FT-IR and DTA-TG-EGA, the hardened $A–C_7A_3Z–H$ paste was ground and the reaction was stopped by cold acetone [20].

Preparation of the Al_2O_3-based refractory composite and methods of investigation

The study of the reaction behaviour of high-temperature synthesis of alumina-based refractory ceramic was analyzed in the $CaO-Al_2O_3-ZrO_2$ system. The pressed cylinders formed from the hydrated paste ($A-C_7A_3Z-H$) were sintered in the electric furnace at a temperature of 1500°C for 10 h with a heating rate of 2°C·min^{-1}. The microstructure and pore size distribution of the sintered samples were examined by Scanning Electron Microscopy (SEM) using the FEI NOVA NANO SEM 200 machine and mercury porosimetry with the PoreMaster 60 Quantachrome, respectively. The samples were also ground to fine powder and analyzed by XRD and FT-IR methods.

RESULTS AND DISCUSSION

Characterization of the starting materials

Figure 1 depicts the XRD pattern of the $Ca_7ZrAl_6O_{18}$ sample sintered at 1500°C for 10 h. The $Ca_7ZrAl_6O_{18}$ is confirmed by comparing the observed XRD pattern with the International Centre for Diffraction Data (ICDD) pattern (No. 98-015-7989). The remaining of the small XRD peaks are ICDD-traced to be residual $CaZrO_3$ phase are in agreement with the ICDD No 98-009-7466. XRD experiments at room temperature revealed that the commercially available hydratable alumina does not contain any impurity phases. All the XRD peaks were completely ICDD-matched, thus confirmed to be those of a single-phase Al_2O_3 (No 01-078-2426). Particle size distribution (PSD) of the cementitious materials i.e. reactive alumina and calcium zirconium aluminate ($Ca_7ZrAl_6O_{18}$), was characterized by the median ($d_{0.5}$) which corresponds to 0.3 μm and 3.4 μm, respectively.

The reactive alumina-$Ca_7ZrAl_6O_{18}$ anhydrous and hydra-ting mixtures were prepared basing on powders with monomodal size distribution.

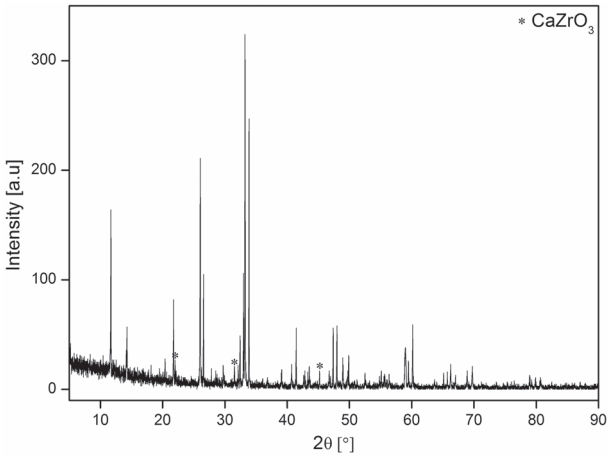

Figure 1. The XRD pattern of the synthesized $Ca_7ZrAl_6O_{18}$.

X-ray diffraction (XRD) and FT-IR studies of the reactive alumina-$Ca_7ZrAl_6O_{18}$ anhydrous and hydrating mixtures

Figures 2a and b present the measured XRD patterns of the anhydrous mixture of reactive alumina-$Ca_7ZrAl_6O_{18}$ and hydrated paste, respectively. As shown in Figure 2b, it can be seen that all peaks of $Ca_7ZrAl_6O_{18}$ disappeared on the XRD pattern of the hydrated paste (A-C_7A_3Z-H) due to phase consumption during hydration. At 50°C, the hydration products of $Ca_7ZrAl_6O_{18}$ were the stable cubic phase (hydrogarnet), $Ca_3[Al(OH_6)]_2$ (C_3AH_6) and gibbsite, $Al(OH)_3$. These findings are in very good agreement with our previous results concerning the hydration mechanisms of $Ca_7ZrAl_6O_{18}$ at elevated temperature [18]. In the XRD pattern of the hydrated paste (A–C_7A_3Z–H) (Figure 2b), reflections for unhydrated Al_2O_3 and some reflections for newly for-med calcium zirconate, $CaZrO_3$ were identified. $CaZrO_3$ formation during hydration of $Ca_7ZrAl_6O_{18}$ was also reported in the literature [16-19].

The FT-IR analyses of dry and hydrated Al_2O_3 and $Ca_7ZrAl_6O_{18}$ phases have been extensively reported in the literature [16, 21-22]. However, these studies have focused on hydration behaviour of these cementitious materials at room temperature, but have not at elevated temperature. The FT-IR data of dry and hydrated mixtures of cementitious materials are illustrated in Figure 3. Basing on IR analysis it can be noted that the infrared spectrum of the unhydrated form of the Al_2O_3–$Ca_7ZrAl_6O_{18}$ mixture (Figure 3a), compared to the spectra from the hydrated mixture (Figure 3b), exhibit significant differences.

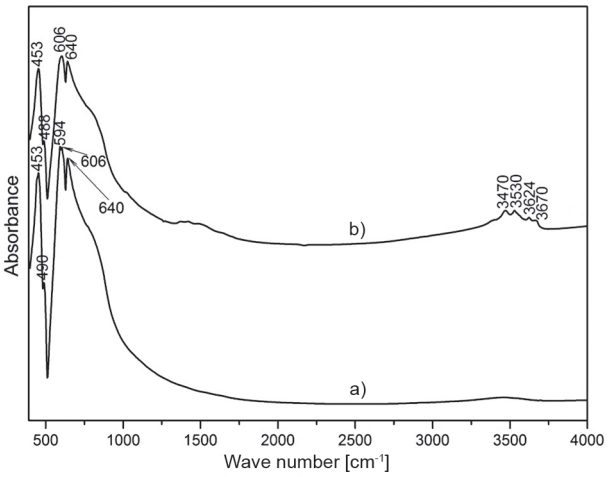

Figure 3. FT-IR spectra of the Al_2O_3–$Ca_7ZrAl_6O_{18}$ mixtures before (a) and after hydration (b) in the range of 400-4000 cm^{-1}.

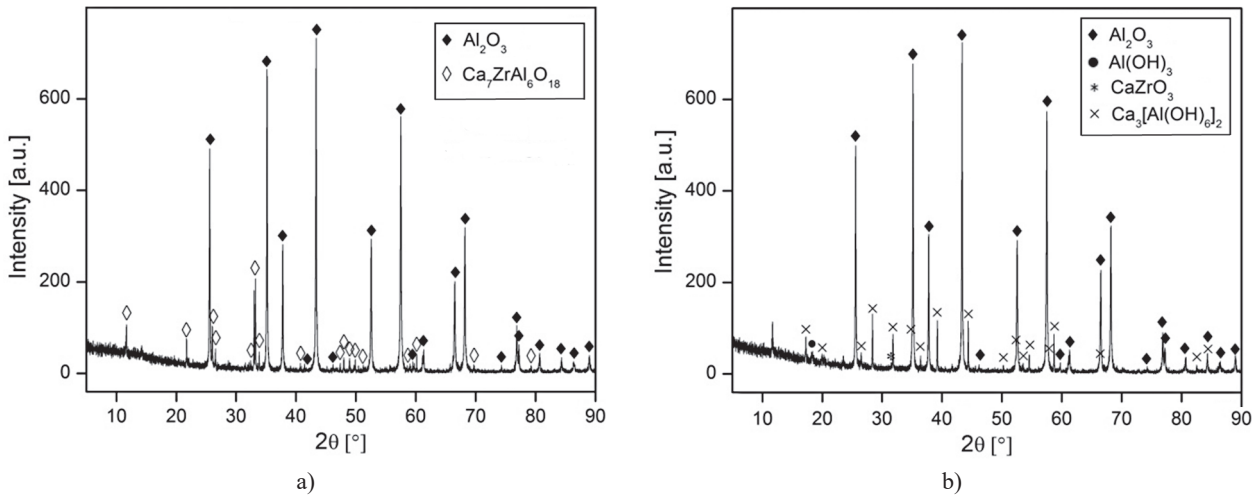

Figure 2. The XRD patterns of the Al_2O_3–$Ca_7ZrAl_6O_{18}$ an-hydrous (a) and hydrated (b) mixtures.

The absorption bands appearing at about 453, 490 or 488, 606 and 640 cm^{-1} in FT-IR spectra of both dry and hydrated mixtures of cementitious materials are attributed to α-Al_2O_3 (Figure 3a and b).The IR bands of α-Al_2O_3 have been assigned according to the study of Tarte [21]. It is interesting to note that major bands of $Ca_7ZrAl_6O_{18}$, appearing in the 580 to 840 cm^{-1} region [16], have disappeared completely after hydration. The $Ca_7ZrAl_6O_{18}$ hydration with water gives up to the development of calcium aluminate hydrates [15-19]. At 50°C or above; the formation of C_3AH_6 and gibbsite is virtually immediate [13] and it was also reported in our previous work [18]. The FT-IR spectrum of the A–C_7A_3Z–H hydrated paste has a very broad band due to the O–H groups in the 3000 - 4000 cm^{-1} region [23] (Figure 3b). This spectrum has bands sited at 3470, 3530 and 3624 cm^{-1} due to the polymorph of aluminium hydroxide, gibbsite, $Al(OH)_3$ and OH-free absorption band at the 3670 cm^{-1} wavenumber of due to C_3AH_6 [22].

Analysis of thermal dehydration of the reactive alumina-$Ca_7ZrAl_6O_{18}$ hydrated mixture by DTA-TG-EGA

The DTA, TG and EGA curves of thermal decomposition of the hydrated paste of cementitious materials are shown in Figure 4. The dehydration processes occur in the temperature range 30 - 1000°C and are registered on the DTA curve as three endothermic peaks with maxima at 87, 252 and 297°C, respectively. A broad endothermic reaction with a peak at 87°C, accompanied by a slow mass loss (1.14 %), due to decomposition of AH_3-gel [24, 25], was observed on the TG curve. According to Day and Lewis [26] or Bushnell-Watson and Sharp [27] the amorphous or micro-crystalline aluminium hydroxide gel may be fully decomposed as high as 200°C or 300°C. The two endothermic DTA effects occurring between 240 and 330°C are associated with the decomposition of crystalline phases, i.e. $Al(OH)_3$ and C_3AH_6 [18, 24]. The maximum at 252°C (DTA) accompanied by 1.37 % mass loss (DTG data; 2.51 % TG data) is attributed to dehydration of $Al(OH)_3$ [24]. The third endothermic peak in the DTA spectra at 297°C and a weight loss of 1.25 % (DTG data; 3.76 % TG data) could be ascribed to dehydration of C_3AH_6. According to Cardoso et al [24] C_3AH_6 may be fully decomposed as high as 370°C. A further gradual mass loss of 2.23 % completed at 1000°C (DTG data; 5.99 % TG data) was due to the decomposition of residual A–H or C–A–H phases. Evolution of H_2O shows a parallel run to the DTA curve having sharp local maxima at the similar temperature values, 247 and 287°C, connected with the decomposition of $Al(OH)_3$ and C_3AH_6, respectively.

Investigations of the alumina-based dense composite

X-ray diffraction (XRD) and FT-IR studies

The XRD pattern of the Al_2O_3-based refractory composite sintered at 1500°C is given in Figure 5. X-ray diffraction experiments indicate that the product of sintering at 1500°C for 10 h consists mainly of α-Al_2O_3, $CaAl_{12}O_{19}$ and the secondary monoclinic polymorph of zirconia. It can be concluded that the lime-rich calcium aluminates, especially $Ca_{12}Al_{14}O_{33}$ ($C_{12}A_7$) [19], formed as dehydration products formed on continuous firing of the A-C_7A_3Z-H green humid sample, reacted with an excess of Al_2O_3 to form the alumina-rich phase, such as $CaAl_{12}O_{19}$ (CA_6). As it has been reported by Vishista and Gnanam in Ref. [28] and Singh in Ref. [29], CA_6 may be formed by the reaction between C and A; the reaction between CA_2 and A; the reaction among CA, CA_2 and A. According to the phase diagram for the CaO-ZrO_2-Al_2O_3 system, proposed by Berezhnoy and Kordyuk [14], calcium zirconate $CaZrO_3$ formed during the hydration reaction of $Ca_7ZrAl_6O_{18}$, coexists with $CaAl_2O_4$ and $CaAl_4O_7$, but not with $CaAl_{12}O_{19}$.

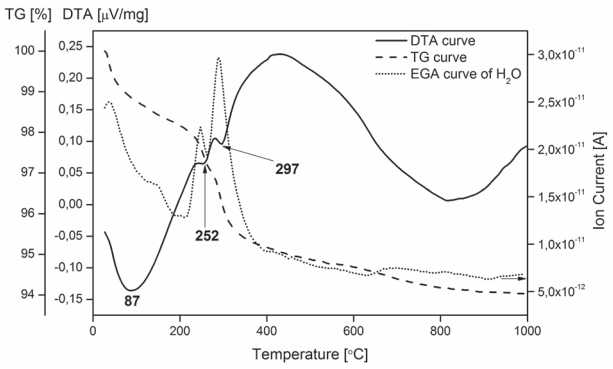

Figure 4. TG/DTA/EGA profiles of the Al_2O_3–$Ca_7ZrAl_6O_{18}$ hydrated mixture cured at 50°C for 14 days.

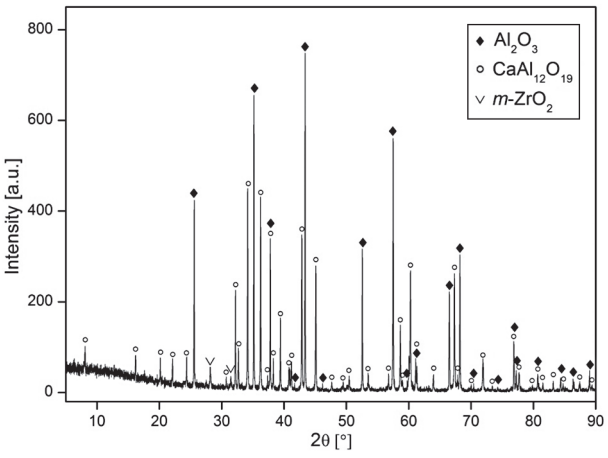

Figure 5. The XRD pattern of the Al_2O_3–$CaAl_{12}O_{19}$–ZrO_2 ceramic composite material.

The Al_2O_3–$CaAl_{12}O_{19}$–ZrO_2 elementary compatibility triangle was found in the CaO-ZrO_2-Al_2O_3 system. Therefore, the chemical reaction between $CaZrO_3$ and Al_2O_3, given by Eq. (1) occurred.

$$CaZrO_3 + 6Al_2O_3 \rightarrow CaAl_{12}O_{19} + ZrO_2 \quad (1)$$

The FT-IR studies have been used to confirm the formed compound. The spectrum of the Al_2O_3-based refractory composite is presented in Figure 6. As it was investigated by Tarte [21], the characteristic frequency ranges of inorganic aluminate phases are as follows: "condensed" AlO_4 tetrahedra in the spectral range of 900 - 700 cm^{-1}, "isolated" AlO_4 tetrahedra (800 - 650 cm^{-1}), "condensed" AlO_6 octahedra (680 - 500 cm^{-1}) and "isolated" AlO_6 octrahedra (530 - 400 cm^{-1}). Corundum α-Al_2O_3 is a representative compound of the "condensed" AlO_6 octahedra category. As it can be seen from Figure 6, the strong absorption bands due to AlO_6 octahedra are centered near 640 and 604 cm^{-1} [21]. This spectrum has also bands centered at about 465, 528, 552, 618, 704, and 777 cm^{-1}, due to synthetic calcium hexaaluminate, $CaAl_{12}O_{19}$ (CA_6) [30]. One additional absorption band centered at about 739 cm^{-1} is distinctive for the monoclinic ZrO_2 polymorph [31].

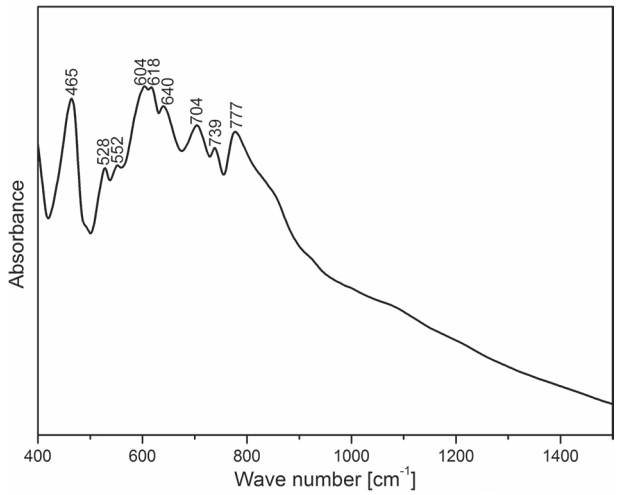

Figure 6. FT-IR spectra of the Al_2O_3–$CaAl_{12}O_{19}$–ZrO_2 ceramic composite material.

SEM/EDS observations

Figures 7 and 8 present the scanning electron microscope image of both polished and fractured sections of the Al_2O_3-based refractory composite sintered at 1500°C. SEM image of polished sections from the sintered Al_2O_3-based ceramic material shows calcium hexaaluminate (Figure 7 – point 1), dispersed as a reinforcing phase in the alumina matrix (Figure 7 – point 2) with a homogeneous distribution of zirconia grains (Figure 7 – point 3). SEM of the fracture section of a sample shows the elongated grain morphology of CA_6 while the alumina grains are small and irregular (Figure 8). The performed microstructure observations using the scanning electron microscope as well performed quantitative X-ray analysis confirm the presence of Al_2O_3, $CaAl_{12}O_{19}$ and ZrO_2, detected by XRD and FT-IR analysis.

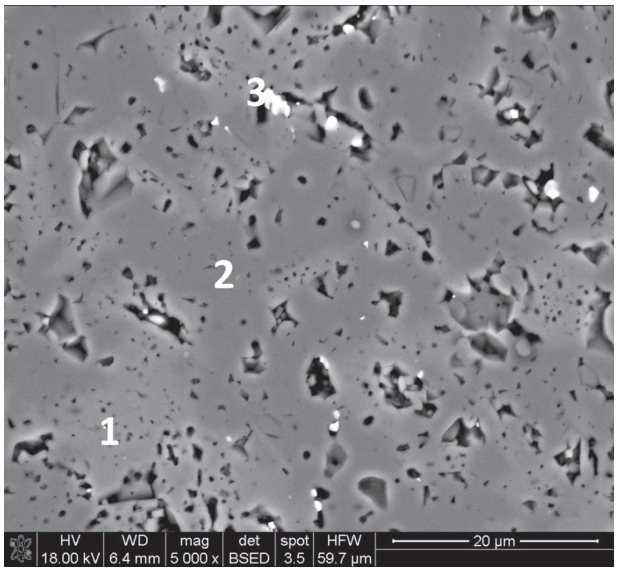

Figure 7. SEM photomicrograph of the polished section of the Al_2O_3–$CaAl_{12}O_{19}$–ZrO_2 ceramic composite material. (Spots 1-3) EDS analysis: 1 – $CaAl_{12}O_{19}$, 2 – Al_2O_3, 3 – ZrO_2.

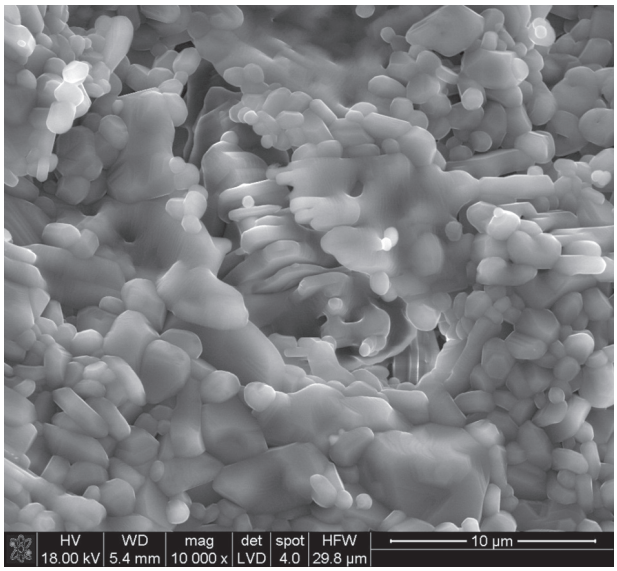

Figure 8. SEM photomicrograph of the fractured section of the Al_2O_3–$CaAl_{12}O_{19}$–ZrO_2 ceramic composite material.

Mercury intrusion porosimetry

The Al_2O_3–$CaAl_{12}O_{19}$–ZrO_2 refractory composite material has a multi-modal pore size distribution, with the pore diameters of 0.004 µm, 0.09 µm, 0.14 µm, 0.24 µm, 0.41 µm, 7.10 µm and 10.19 µm.

The predominant pore size is centered around 0.41 μm. For this composite, the average open porosity, as determined by mercury intrusion porosimetry, was 13.3 %. The pore size characteristics of the Al_2O_3–$CaAl_{12}O_{19}$–ZrO_2 composite are presented by pore size distribution both in the form of differential and cumulative pore size distribution and are shown in Figures 9 and 10, respectively.

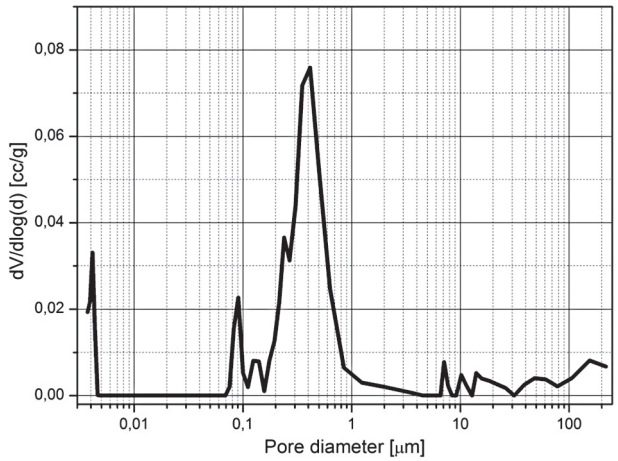

Figure 9. Differential pore size distribution curve for the Al_2O_3–$CaAl_{12}O_{19}$–ZrO_2 ceramic composite material.

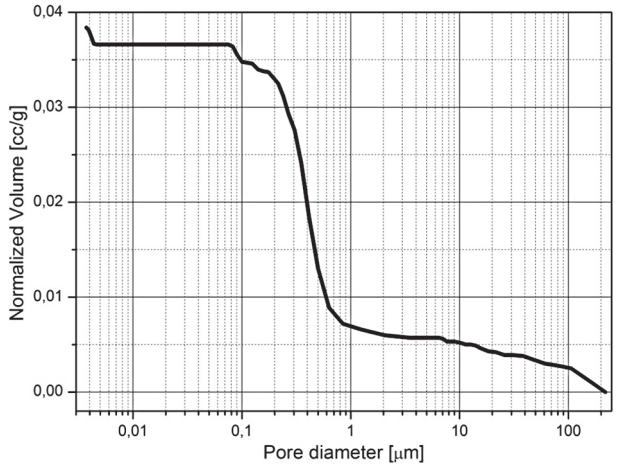

Figure 10. Cumulative pore size distribution curves the Al_2O_3–$CaAl_{12}O_{19}$–ZrO_2 ceramic composite material.

CONCLUSIONS

The subject of this paper was to characterize the reaction and phases from the hydratable materials: reactive alumina (Al_2O_3) and calcium zirconium aluminate ($Ca_7ZrAl_6O_{18}$) at 50°C and 1500°C. Our investigations concerned the transformation of hydraulic bonding in the hydrated mixture of Al_2O_3 and $Ca_7ZrAl_6O_{18}$ into calcium hexaaluminate, acting as a ceramic bonding phase in the alumina-based ceramic material. For this purpose DTA-TG-EGA, XRD, FT-IR and SEM/EDS techniques were employed.

Products of the hydrated mixture of Al_2O_3 and $Ca_7ZrAl_6O_{18}$ were studied by X-ray diffractions (XRD), thermal analysis (TG-DTA-TG) and Fourier transform infrared spectroscopy (FT-IR) after 14 days of curing and hydration at 50°C. According to these results, the thermodynamically stable crystalline hydrates, i.e. C_3AH_6 and $Al(OH)_3$, were formed at 50°C.

Calcium zirconate $CaZrO_3$, also formed during the hydration process of $Ca_7ZrAl_6O_{18}$ and the lime-rich calcium aluminates, formed upon dehydration of C_3AH_6, were not stable and reacted with Al_2O_3 to form monoclinic zirconia and calcium hexaaluminate, respectively. The presence of *m*-ZrO_2 and $CaAl_{12}O_{19}$ was confirmed by XRD and FT-IR. A microstructural examination of the Al_2O_3-based ceramic showed a dense structure with dispersion of the reinforcement of the calcium hexaaluminate phase with a homogeneous distribution of zirconia grains. The heterogeneous pore size distribution of the Al_2O_3–$CaAl_{12}O_{19}$–ZrO_2 ceramic composite material with the predominant pore size centered at 0.41 μm was identified. Characterization of the reaction in the Al_2O_3–$Ca_7ZrAl_6O_{18}$–H_2O system, its dehydration behavior and phase changes are important from the point of view of possible applications of $Ca_7ZrAl_6O_{18}$ in high alumina castables technology.

Acknowledgments

This work is supported by the grant no INNOTECH-K2/IN2/16/181920/NCBR/13 of the National Centre for Research and Development.

The authors thank Alteo NA LLC company for supplying reactive alumina to complete this study.

REFERENCES

1. Jerebtsov D.A, Mikhailov G.G. (2001): Phase diagram of CaO-Al_2O_3 system. *Ceramics International*, *27*(1), 25-28. doi:10.1016/S0272-8842(00)00037-7
2. Iftekhar S., Grins, J. Svensson G., Lööf J., Jarmar T., Botton G.A., Andrei C.M., Engqvist H. (2008): Phase formation of $CaAl_2O_4$ from $CaCO_3$-Al_2O_3 powder mixtures. *Journal of the European Ceramic Society*, *28*(4), 747-756. doi:10.1016/j.jeurceramsoc.2007.08.012
3. Rivas Mercury J.M., De Aza A.H., Pena P. (2005): Synthesis of $CaAl_2O_4$ from powders: Particle size effect. *Journal of the European Ceramic Society*, *25*(14), 3269-3279. doi:10.1016/j.jeurceramsoc.2004.06.021
4. Tchamba A.B., Melo U.C., Lecomte-Nana G.L., Kamseu E., Gault C., Yongue R., Njopwouo D. (2014): Use of bauxite from Cameroon for solid state sintering and characterization of calcium dialuminate ($CaO{\cdot}2Al_2O_3$) refractory cement. *Ceramics International*, *40*(1), 1961-1970. doi:10.1016/j.ceramint.2013.07.105
5. Scrivener K.L., Cabiron J.-L., Letourneux R. (1999): High-

performance concretes from calcium aluminate cements. *Cement and Concrete Research*, *29*(8), 1215-1223. doi:10.1016/S0008-8846(99)00103-9
6. Gogtas C., Lopez H.F., Sobolev K. (2014): Role of cement content on the properties of self-flowing Al_2O_3 refractory castables. *Journal of the European Ceramic Society*, *34*(5), 1365-1373. doi:10.1016/j.jeurceramsoc.2013.11.004
7. Zherebtsov D.A., Archugov S.A., Mikhailov G.G. (1999): Fusibility of the CaO–Al_2O_3 System *Rasplavy*, *2*, 63-65.
8. Klaus S.R., Neubauer J., Goetz-Neunhoeffer F. (2013): Hydration kinetics of CA_2 and CA – Investigations performed on a synthetic calcium aluminate cement. *Cement and Concrete Research*, *43*, 62-69. doi:10.1016/j.cemconres.2012.09.005
9. Ukrainczyk N. (2010): Kinetic modeling of calcium aluminate cement hydration. *Chemical Engineering Science*, *65*(20), 5605-5614. doi:10.1016/j.ces.2010.08.012
10. Mostafa N.Y., Zaki Z.I., Abd Elkader O.H. (2012): Chemical activation of calcium aluminate cement composites cured at elevated temperature. *Cement and Concrete Composites*, *34*(10), 1187-1193. doi:10.1016/j.cemconcomp.2012.08.002
11. Griffin J.G., Daugherty K.E. (1985): The effect of temperature on the hydration of the calcium aluminates at high water-solid ratios. *Thermochimica Acta*, *91*(1), 53-60. doi:10.1016/0040-6031(85)85200-X
12. Odler I. (2000). Special Inorganic Cements (Modern Concrete Technology). CRC Press.
13. Taylor H.F.W. (1997).Cement Chemistry. 2nd ed. Thomas Telford, London.
14. Berezhnoi A.S., Kordyuk R.A. (1963): Melting diagram of the system CaO-Al_2O_3-ZrO_2. *Dopovidi Akademii Nauk Ukrainskoi RSR*, *10*, 1344-1347.
15. Fukuda K., Iwata T., Nishiyuki K. (2007): Crystal structure, structural disorder, and hydration behavior of calcium zirconium aluminate, $Ca_7ZrAl_6O_{18}$. *Chemistry of Materials*, *19*(15), 3726-3731. doi:10.1021/cm070731z
16. Madej D., Szczerba J., Nocuń-Wczelik W., Gajerski R. (2012): Hydration of $Ca_7ZrAl_6O_{18}$ phase. *Ceramics International*, *38*(5), 3821-3827. doi:10.1016/j.ceramint.2012.01.031
17. Szczerba J., Madej D., Śnieżek E., Prorok R. (2013): The application of DTA and TG methods to investigate the non-crystalline hydration products of $CaAl_2O_4$ and $Ca_7ZrAl_6O_{18}$ compounds. *Thermochimica Acta*, *567*, 40-45. doi:10.1016/j.tca.2013.01.031
18. Madej D., Szczerba J., Nocuń-Wczelik W., Gajerski R., Hodur K. (2013): Studies on thermal dehydration of the hydrated $Ca_7ZrAl_6O_{18}$ at different water-solid ratios cured at 60°C. *Thermochimica Acta*, *569*, 55-60. doi:10.1016/j.tca.2013.07.011
19. Szczerba J., Madej D., Dul K., Bobowska P. (2014): $Ca_7ZrAl_6O_{18}$ acting as a hydraulic and ceramic bonding in the MgO-$CaZrO_3$ dense refractory composite. *Ceramics International*, *40*(5), 7315-7320. doi:10.1016/j.ceramint.2013.12.073
20. Luz A.P., Pandolfelli V.C. (2011): Halting the calcium aluminate cement hydration process. *Ceramics International*, *37*(8), 3789-3793. doi:10.1016/j.ceramint.2011.06.034
21. Tarte P. (1967): Infra-red spectra of inorganic aluminates and characteristic vibrational frequencies of AlO_4 tetrahedra and AlO_6 octahedra. *Spectrochimica Acta Part A: Molecular Spectroscopy*, *23*(7), 2127-2143. doi:10.1016/0584-8539(67)80100-4
22. Fernández-Carrasco L., Torrens-Martín D., Morales L.M., Martínez-Ramírez S. (2012): Infrared Spectroscopy in the Analysis of Building and Construction Materials, in: Theophanides T. (ed.): *Infrared Spectroscopy – Materials Science, Engineering and Technolog.* InTech, ISBN: 978-953-51-0537-4, available from: http://www.intechopen.com/books/infrared-spectroscopy-materials-science-engineering-and-technology/infrared-spectroscopy-of-cementitious-materials. doi: 10.5772/36186
23. Torréns-Martín D., Fernández-Carrasco L., Martínez-Ramírez S. (2013): Hydration of calcium aluminates and calcium sulfoaluminate studied by Raman spectroscopy. *Cement and Concrete Research*, *47*, 43-50. doi:10.1016/j.cemconres.2013.01.015
24. Cardoso F.A., Innocentini D.M.M., Akiyoshi M.M., Pandolfelli V.C. (2004): Effect of curing time on the properties of CAC bonded refractory castables. *Journal of the European Ceramic Society*, *24*(7), 2073-2078. doi:10.1016/S0955-2219(03)00371-6
25. George C.M. (1983). Industrial alumina cement, in: Barnes P. (ed.): *Structure and Performance of Cement*.
26. Day D.E., Lewis G. (1979): Quantitative thermogravimetry of calcium aluminate compounds and cements after hydrothermal treatment. *American Ceramic Society Bulletin*, *58*, 441-444.
27. Bushnell-Watson S.M., Sharp J.H. (1985): The detection of the carboaluminate phase in hydrated high alumina cements by differential thermal analysis. *Thermocimica Acta*, *93*, 613-616. doi:10.1016/0040-6031(85)85154-6
28. Vishista K., Gnanam F.D. (2005): Sol-gel synthesis and characterization of alumina-calcium hexaaluminate composites. *Journal of the American Ceramic Society*, *88*(5), 1175-1179. doi: 10.1111/j.1551-2916.2005.00330.x
29. Singh V.K. (1999): Sintering of calcium aluminate mixes. *British Ceramic Transactions, 98*(4), 1213-1216. doi:http://dx.doi.org/10.1179/096797899680426
30. Hofmeister A.M., Wopenka B., locock A.J. (2004): Spectroscopy and structure of hibonite, grossite, and $CaAl_2O_4$: Implications for astronomical environments. *Geochimica et Cosmochimica Acta*, *68*(21), 4485-4503. doi:10.1016/j.gca.2004.03.011
31. Phillippi C.M., Mazdiyasni K.S. (1971): Infrared and Raman spectra of zirconia polymorphs. *Journal of the American Ceramic Society*, *54*(5), 254-258. doi:10.1111/j.1151-2916.1971.tb12283.x